WITHDRAWN: Contribution of microRNA-30d to the prevention of the thyroid cancer progression: mechanism and implications

Yuan Shao
  the First Affiliated Hospital of Xi'an Jiaotong University

Shaoqiang Zhang
  the First Affiliated Hospital of Xi'an Jiaotong University

Xiaoxia Wang
  Air Force 986 Hospital of Chinese People's Liberation Army

Xin Sun
  the First Affiliated Hospital of Xi'an Jiaotong University

Jie Wu
  the First Affiliated Hospital of Xi'an Jiaotong University

Fang Sui
  the First Affiliated Hospital of Xi'an Jiaotong University

Fangli Yang
  the First Affiliated Hospital of Xi'an Jiaotong University

Hao Dai
  the First Affiliated Hospital of Xi'an Jiaotong University

Junsong Liu
  the First Affiliated Hospital of Xi'an Jiaotong University

XiaoBao Yao
  the First Affiliated Hospital of Xi'an Jiaotong University

Honghui Li
  the First Affiliated Hospital of Xi'an Jiaotong University

Lifeng Liu
  the First Affiliated Hospital of Xi'an Jiaotong University

Xuan Wang
  the First Affiliated Hospital of Xi'an Jiaotong University

Zhiwei Zheng
  Rizhao People's Hospital

Chongwen Xu
  xucw-2@163.com

Research

EDITORIAL NOTE:

The full text of this preprint has been withdrawn by the authors while they make corrections to the work. Therefore, the authors do not wish this work to be cited as a reference. Questions should be directed to the corresponding author.

Abstract

Background

Thyroid cancer is a major endocrine tumor and represents an emerging health problem worldwide. MicroRNAs (miRNAs) have been addressed to be associated with the pathogenesis and progression of thyroid cancer. However, it remains largely unknown what functions miR-30d may exert on thyroid cancer. This study herein aimed to identify the functional significance and mechanism of miR-30d in the progression of thyroid cancer.

Methods

The expression of miR-30d and ubiquitin-specific protease 22 (USP22) in cancerous tissues of patients with thyroid cancer was measured using RT-qPCR and Western blot analysis. In response to the gain- or loss-of-function of miR-30d and USP22, cell apoptosis was evaluated by flow cytometry and TUNEL staining in combination with the measurement of apoptosis-related proteins. The interactions among miR-30d, USP22, SIRT1, FOXO3a and PUMA were explored using a series of assays, including dual-luciferase reporter gene assay, Co-IP and ChIP assay. The effects of miR-30d and USP22 on thyroid tumorigenesis were finally validated *in vivo*.

Results

MiR-30b presented aberrant low expression in thyroid cancer tissues and this low expression correlated with poor prognosis of thyroid cancer patients. miR-30d promoted apoptosis of thyroid cancer cells through targeting USP22, an up-regulated gene in thyroid cancer. USP22 could enhance the stability of SIRT1 by inducing deubiquitination which consequently contributed to FOXO3a deacetylation-induced PUMA repression. It was verified that this regulatory mechanism was responsible for the pro-apoptotic effect of miR-30d by the *in vivo* tumorigenicity assay.

Conclusion

To conclude, the progression of thyroid cancer can be suppressed by miR-30d-mediated inhibition of USP22, provides a promising therapeutic target for thyroid cancer treatment.

Background

Thyroid cancer is a life-threatening endocrine tumor and the ninth most common cancer with over 560,000 incident cases in 2018 all over the world estimated by the International Agency for Research on Cancer [1, 2]. Thyroid cancer is characterized by neck lump, difficulty in breathing or swallowing or hoarseness [3]. Based on the histopathological types, thyroid cancer can be classified into papillary

thyroid cancer (PTC), follicular thyroid cancer (FTC), medullary thyroid cancer (MTC) and anaplastic thyroid cancer (ATC) [4, 5]. Most cases of thyroid carcinoma can be treated with local or radical excision, with or without radioactive iodine therapy, external beam radiation and/or chemotherapy [3]. However, optimized prophylactic and therapeutic medications related to the inhibition of cancer cell proliferation is still in urgent demand [6]. MicroRNAs (miRNAs) are small RNAs that modulate numerous cellular processes and increasingly identified as crucial regulators in thyroid tumorigenesis [7, 8]. A former study from Zhang et al has identified the possibility of miR-30d as a potential therapeutic target for ATC [9]. Our study herein was designed to explore the specific functions and molecular mechanisms of miR-30d in thyroid cancer.

Ubiquitin-specific protease 22 (USP22) is a deubiquitinating enzyme which has been reported as a crucial predictor of poor prognosis and a tumor promoter in thyroid cancer [10, 11]. Zhao et al found out that USP22, targeted by miR-101, can exert stimulatory role in the development of PTC [12]. It is reported that sirtuin-1 (SIRT1) is implicated in the development of malignancies by functioning as a mediator of cell growth and apoptosis [13]. SIRT1 has been considered as tumor promoter in thyroid cancer and represents a potential therapeutic target [14], and it was also found to be mediated by miR-30e-5p-repressed USP22, thereby inhibiting the tumorigenesis of non-small cell lung cancer (NSCLC) [15]. Forkhead transcription factor O3a (FoxO3a) is a known suppressor of primary tumor growth in ATC through transcriptional regulation of key genes such as cyclin A1 [16]. More importantly, FoxO3a can be regulated by SIRT1 and thus is implicated in pathogenesis of autoimmune thyroid diseases [17]. In addition, P53-up-regulated modulator of apoptosis (PUMA), a member of Bcl2 family, is identified as an inducer of cell apoptosis [18, 19]. Interestingly, FOXO3a can activate PUMA to facilitate the apoptosis of prostate cancer cells, highlighting the importance of their interaction in tumorigenesis [20]. On the basis of USP22 being predicted to be a key target gene of miR-30d, we hypothesized that miR-30d could modulate the SIRT1/FOXO3a/PUMA axis by mediating USP22 and exert great influence on the development of thyroid cancer. Hence, the present study was conducted for exploration purpose to ultimately provide a novel target to the treatment of thyroid cancer.

Material And Methods

Ethics statement

The current study was performed with the approval of the Ethics Committee of the First Affiliated Hospital of Xi'an Jiaotong University and the procedures conformed to the Declaration of Helsinki. Written informed consent was obtained from each participant. Animal experimental procedures were in strict accordance with recommendations in the Guide for the Care and Use of Laboratory Animals issued by the National Institutes of Health.

Study subjects

Seventy-two cases of cancer tissues (T) of patients with thyroid cancer and the same amount of adjacent normal tissues (N) were obtained from the First Affiliated Hospital of Xi'an Jiaotong University and timely

stored in liquid nitrogen at -80°C for subsequent experiments. All patients were followed up for 5 years or until death.

In silico analysis

We analyzed the expression of key miRNAs of thyroid cancer in microarray GSE97070 gained from Gene Expression Omnibus (GEO) database (https://www.ncbi.nlm.nih.gov/gds), followed by correlation analysis of the miRNAs with the clinical prognosis using starBase (http://starbase.sysu.edu.cn/). The downstream genes of the candidate miRNA were predicted using mirDIP (Integrated Score > 0.65, Number of Sources > 15) (http://ophid.utoronto.ca/mirDIP/), microRNA (energy < -10) (http://www.microrna.org/microrna/home.do), TargetScan (Cumulative weighted context + + score < -0.25, Total context + + score ≦ -0.3) (http://www.targetscan.org/vert_71/), starBase (clipExpNum > 20, pancancerNum > 1) and DIANA TOOLS (miTG score > 0.8) (http://diana.imis.athena-innovation.gr/DianaTools). String (minimum required interaction score: 0.3) (https://string-db.org/) was applied to construct a protein-protein-interaction (PPI) network. The downstream pathways of key genes were determined using starBase, GEPIA (http://gepia2.cancer-pku.cn) and the existing literature.

Cell culture and transfection

Thyroid cancer cell line SW579 purchased from the American Type Culture Collection (ATCC) (https://www.atcc.org/) was cultured in RPMI-1640 medium containing 100 μg/mL streptomycin and 100 U/mL penicillin (Gibco BRL, Grand Island, NY, USA) at 37°C with 5% CO_2 and 95% O_2. Cells were treated with 0.25% trypsin and passaged in an amount of 1 : 3. Cells in logarithmic growth phase were obtained and seeded into a 6-well plate (3×10^5 cells/well). When the cell confluence reached 70−80%, the cells were transfected using Lipofectamin 3000 (L3000008, Invitrogen, Carlsbad, CA). The sequences and plasmids (GenePharma, Shanghai, China) for cell transfection included mimic-negative control (NC), miR-30d mimic, small interfered RNA (si)-NC, si-USP22-1, si-USP22-2, si-SIRT1-1, si-SIRT1-2, si-FOXO3a-1, si-FOXO3a-2, overexpressed (oe)-NC, oe-USP22, and oe-FOXO3a. After 48-h transfection, cells were collected for subsequent experiments.

Dual-luciferase reporter gene assay

The biological prediction website (microRNA.org) was used for predict the binding sites of miR-30d on USP22 3'UTR, and the luciferase reporter assay was conducted to verify whether USP22 can be regulated by miR-30d. After 12−16 h incubation of SW579 cells in 35 mm culture dishes, the artificially synthesized USP22 3'UTR gene fragment was introduced into the pMIR-reporter plasmid using the endonuclease sites SpeI and Hind III (Beijing Huayueyang Biotechnology Co., Ltd., Beijing, China). The complementary sequence containing mutation (MUT) binding site was designed based on USP22 wild type (WT) sequence and inserted into pMIR-reporter plasmid using T4 DNA ligase. The sequenced WT and MUT luciferase reporter plasmids were co-transfected into HEK-293T cells with miR-30d mimic. After 48 h, cells were collected and protein were extracted. The luciferase activity was assayed by luciferase detection kit (K801-200, Biovision Milpitas, CA) in a Lomax20/20 luminometer (Promega, Madison, WI). The activity of SIRT1 binding to FOXO3a promoter was also tested using the same method.

Flow cytometry

The cells in the culture dish were treated with ethylenediaminetetraacetic acid (EDTA)-free trypsin and collected. The cell supernatant was collected after centrifugation at 2000 rpm for 5 min. The collected cell supernatant were washed twice with phosphate buffered saline (PBS) and stained with 5 μL of Annexin-V-fluorescein isothiocyanate (FITC) and 5 μL of propidium iodide (PI) (KGA106, KGI) for 15 min, and cell apoptosis was then detected by a flow cytometer (BD Biosciences, San Jose, CA).

Cell counting-kit 8 (CCK-8) assay

Cells were seeded into a 96-well plate at a density of 2×10^4 cells/well. After transfection, the cells were treated with 10 μL per well of CCK-8 reagent (Dojindo, Kumamoto, Japan) for $1-4$ h. The optical density (OD) value at 450 nm of each well was detected using a microplate reader (Bio-Rad, Hercules, CA).

Terminal deoxynucleotidyl transferase-mediated deoxyuridine triphosphate (dUTP)-biotin nick end labeling (TUNEL) staining

The cells in 24-well plate were rinsed 3 times with PBS, fixed with 4% paraformaldehyde for 30 min, and fixed with 0.3% H_2O_2-formaldehyde solution (30% H_2O_2; formaldehyde = 1 : 99) for 30 min, successively. The cells were treated with 0.3% Triton X-100 on ice for 2 min, and rinsed 3 times with PBS. TUNEL reaction mixed solution was prepared using TUNEL apoptosis detection kit (green fluorescence, C1088, Beyotime). The cells to be tested were treated with 50 μL TdT + 450 μL fluorescein-labeled dUTP solution, and the cells in the NC group was treated only with 50 μL fluorescein-labeled dUTP solution. Then cells were incubated at 37^oC for 60 min in the dark, and then rinsed 3 times with PBS or Hank's balanced salt solution. After being sealed with an anti-fluorescence quenching mounting solution, cells were observed under a fluorescence microscope. The signals were detected at excitation wavelength of 450 nm and emission wavelength of 550 nm (green fluorescence). TUNEL staining for tumor tissues was conducted with the same procedures as above.

Reverse transcription quantitative polymerase chain reaction (RT-qPCR)

Total RNA was extracted using TRIzol kit (Thermo Fisher Scientific, Waltham, MA), and 5 μg RNA was reverse-transcribed into cDNA with a RT-qPCR kit (ABI Company, Oyster Bay, NY). A total of 25 μL reaction system was used for PCR amplification of the target gene, including 300 ng cDNA, 1 × PCR buffer, 200 μmol/L dNTPs, 80 pmol/L for each of the forward and reverse primers, and 0.5 U Taq enzyme (S10118, Shanghai yuanye Bio-Technology Co., Ltd, Shanghai, China). Primers used for RT-qPCR were as presented in Table 1. U6 was used as the internal reference for miR-30d and glyceraldehyde-3-phosphate dehydrogenase (GAPDH) as internal reference primer for other genes. The relative expression of experimental group genes and control group genes was calculated using $2^{-\triangle\triangle CT}$ method: $\triangle\triangle Ct = \triangle Ct$

(experimental group) - $\triangle$Ct (control group), $\triangle$Ct = Ct (target gene) - Ct (internal reference), relative transcription level = $2^{-\triangle\triangle Ct}$.

Table 1
Primer sequence for RT-qPCR

Gene	Species	Primer sequence
miR-30d	human	F: 5'-TAAACATCCCCGACTG-3
		R: 5'-AACTGGTGTCGTGGAG-3'
USP22	human	F: 5'-GGCCAATTGGCCTTGGAAATCTGCCCCTTAT-3'
		R: 5'-CGGTTAGGATTACGGTTAACTTGTTCA-3'
SIRT1	human	F: 5'-AGGATAGAGCCTCACATGCAA-3'
		R: 5'-TCGAGGATCTGTGCCAATCATA-3'
FOXO3a	human	F: 5'-TCACGCACCAATTCTAACGC-3'
		R: 5'-CACGGCTTGCTTACTGAAGG-3'
PUMA	human	F: 5'-AGACAAGAAGAGCAGCATCGACAC-3'
		R: 5'- TAGGCACCTAGTTGGGCTCCATTT-3'
U6	human	F: 5'-GCTTCGGCAGCACATATACTAAAAT-3'
		R: 5'-CGCTTCAGAATTTGCGTGTCAT-3'
GAPDH	human	F: 5'-TGA AGGTCGGAGTCAACGG-3'
		R: 5'-CTGGAAGATGGTGATGGGATT-3'

Note: RT-qPCR, Reverse transcription quantitative polymerase chain reaction; miR-30d, microRNA-30d; USP22, ubiquitin-specific protease 22; SIRT1, sirtuin-1; FOXO3a, Forkhead box protein O3; PUMA, p53-up-regulated modulator of apoptosis; GAPDH, glyceraldehyde-3-phosphate dehydrogenase; F, forward; R, reverse.

Western blot analysis

Cells were washed with PBS and lysed with cell lysis buffer (P0013, Beyotime). Tissues were grinded in liquid nitrogen, lysed with cell lysis buffer (P0013, Beyotime) and incubated at 4°C for 30 min (shaking every 10 min). The cell lysate was centrifuged in an 1.5 mL eppendorf (EP) tube at 12,000 g at 4°C for 15 min, and the supernatant was collected. The protein concentration was determined by bicinchoninic acid (BCA) protein concentration assay kit (Beyotime). The protein loading buffer was added to the supernatant. After boiling for 5 min, 20 µg of the protein sample was electrotransferred to a polyvinylidene fluoride (PVDF) membrane by 10% sodium dodecyl sulfate polyacrylamide gel electrophoresis (Millipore, Billerica, MA, USA) at 0.3 A, 20 V. The membrane was blocked with 5% skimmed milk powder for 1 h, and incubated with primary antibodies as follow: Tris Buffered Saline with

Tween (TBST)-diluted USP22 (ab195289, 1 : 2000, Rabbit, Abcam, Cambridge, UK), SIRT1 (ab32441, 1 : 20000, Rabbit, Abcam), FOXO3a (ab12162, 1 : 2500, Rabbit, Abcam), FOXO3a (acetyl lysine) (ab21623, 1 : 500, Rabbit, abcam), PUMA (ab9643, 1 : 1000, Rabbit, Abcam), flag [# 14793, 1 : 600, Rabbit, Cell Signaling Technology (CST), Danvers, MA, USA], Ubiquitin (# 3936, 1: 1000, Mouse, CST), Caspase-3 (ab13847, 1 : 500, Rabbit, Abcam), Cleaved-caspase-3 (ab179517, 1 : 1000, Rabbit, Abcam), Bcl-2 associated X (Bax, ab32503, 1 : 2000, Rabbit, Abcam), and B cell leukemia/lymphoma 2 (Bcl-2, ab182858, 1 : 2000, Rabbit, Abcam) at 4°C overnight. The membrane was incubated with horseradish peroxidase (HRP)-labeled IgG secondary antibody (ab205718, goat anti-rabbit, 1 : 10000; ab205719, goat anti-mouse, 1 : 10000, Abcam) for 1 h at room temperature, and developed by enhanced chemiluminescence (ECL; Shanghai Baoman Bio-technology Co., Ltd., Shanghai, China). The glyceraldehyde-3-phosphate dehydrogenase (GADPH) antibody (ab181602, 1 : 10000, Rabbit, Abcam) was applied as an internal reference, and the gray value of each band was analyzed using Image J software.

Co-immunoprecipitation (Co-IP) assay

The flag-labeled plasmids were transfected into SW579 cells. After 48 h, the cells were collected for total protein extraction and the total protein was quantified by BCA method. 30 µL of flag antibody-conjugated resin was added to 1 mg of total protein and incubated overnight at 4°C with shaking. The supernatant was then discarded after centrifugation and the pellets were denatured. The protein was transferred to the PVDF membrane by agarose gel electrophoresis, and the primary antibodies utilized for Western blots were anti-SIRT1 (ab32441, 1 : 30, Rabbit, Abcam), anti-FOXO3a (ab12162, 1 : 600, Rabbit, Abcam) and anti-flag (# 14793, 1 : 50, Rabbit, CST).

Protein stability detection

After 48-h of transfection, cells were incubated with CHX (10 µg/mL, HY-12320, MedChem Express, Monmouth Junction, NJ) or MG132 (10 µmol/L, HY-13259, MedChem Express) at 37°C for 0, 1, 2, and 4 h, respectively. Cells were harvested for protein extraction, SIRT1 expression in the extracted protein was measured by Western blots, and SIRT1 degradation curve was plotted.

Ubiquitination assay

After 48 h of transfection, SW579 cells were incubated with MG132 (10 µmol/L) for 6 h. After MG132 treatment, the cells were collected for total protein extraction. 20 µg of the protein sample was electrotransferred to a PVDF membrane by 10% SDS-PAGE (Millipore) at 0.3 A, 20 V. The membrane was blocked with 5% skimmed milk powder for 1 h and incubated with anti-SIRT1 (ab32441, 1 : 20000, Rabbit, Abcam) and TBST-diluted anti-Ub (# 3936, 1 : 1000, Mouse, CST), respectively, at 4°C overnight. Then membrane was incubated with HRP-labeled secondary antibody (ab205718, goat anti-rabbit, 1 : 10000; ab205719, goat anti-mouse, 1 : 10000. Abcam) at room temperature for 1 h, and developed by ECL (Shanghai Baoman Bio-technology Co., Ltd.). The gray value of each band normalized to GADPH was analyzed using the software Image J.

Chromatin immunoprecipitation (ChIP) assay

The enrichment of FOXO3a in the PUMA promoter region was determined by ChIP assay using an EZ-Magna ChIP TMA kit (Millipore). SW579 cells were cross-linked in 1% formaldehyde for 10 min, and then cultured with 125 mM glycine for 5 min to terminate the cross-linking. The cells were washed twice with pre-chilled PBS and centrifuged at 2000 rpm for 5 min. The cells were resuspended in cell lysis buffer [150 mM NaCl, 50 mM Tris (pH 7.5), 5 mM EDTA, 0.005% NP40, 0.01% Triton X-100] to reach a final cell concentration at 2×10^6 cells per 200 mL. The cells were added with protease inhibitor mixture and centrifuged at 5000 rpm for 5 min, followed by resuspension with nuclear separation buffer. The cells were lysed in ice water bath for 10 min and sonicated to obtain 200−1000 bp chromatin fragments. The fragments were then centrifuged at 14000 g at 4°C for 10 min. A total of 100 μL (DNA fragments) supernatant were incubated with 900 μL ChIP dilution buffer, 20 μL of 50 × PIC, and 60 μL of ProteinA Agarose/Salmon Sperm DNA each at 4 °C for 1 h. The cells were then allowed to stand at 4 °C for 10 min and centrifuged at 700 rpm for 1 min, and 20 μL of the supernatant were taken as input. The experimental supernatant was treated with 1 μL antibody to FOXO3a (ab12162, 1: 50 − 1 : 600, Rabbit, Abcam), while 1 μL of rabbit anti-IgG (ab172730, Abcam) was utilized as NC. Afterwards, the DNA-antibody complex was rotated with 60 μL of Protein A Agarose/Salmon Sperm DNA at 2 °C for 2 h. The pellet harvested after centrifugation was rinsed with 1 mL of low-salt buffer, high-salt buffer, LiCl solution, and TE (twice) in order, and was eluted twice with 250 mL ChIP wash buffer. The complex was de-crosslinked with 20 mL NaCl, and DNA was harvested after de-crosslinking. The promoter sequence of PUMA (F: 5'-TTGTGACATGTGTGGGTGGT-3'; R: 5'-AAGGCCACAGTCTCGCAAAT-3) in the complex was quantified using RT-qPCR.

Xenograft tumor in nude mice

Cells were trypsinized and pipetted to generate cell suspension at the density of 5×10^4 cells/mL and seeded into a 6-well plate (2 mL/well). The SW579 cells were infected with lentiviruses (Hanbio Co., Ltd., Shanghai, China) with the use of polybrene (REVG0001, Shanghai Genechem Co., Ltd., Shanghai, China). The stably infected cells were collected after 48-h of infection at 37 °C.

Cells were mixed with Matrigel after PBS washing, and injected into the left axilla of nude mice subcutaneously at the density of 2×10^6 cells per mouse, 100 μL each mouse. The tumor size was measured on the 3rd d after injection and monitored every 3 d to record the changes in tumor size and volume.

Hematoxylin-eosin (HE) staining

The excised tumors from nude mice were fixed with 4% paraformaldehyde for more than 24 h. After the tissues were embedded with paraffin, the tissue sections were dewaxed and hydrated. The sections were then stained with hematoxylin for 7 min, and rinsed with tap water for 10 min to wash away the excess staining solution. The sections were rinsed with distilled water again, and treated with 95% ethanol for 5 s. After the sections were stained with eosin for 1 min, the sections were hydrated with gradient ethanol,

transparentized with xylene (5 min × 2 times), air-dried in a fume hood and sealed with neutral gum. The morphological changes were observed under a light microscope.

Statistical analysis

All experimental data were analyzed using SPSS 21.0 statistical software (IBM Corp, Armonk, NY, USA). Measurement data were all expressed as mean ± standard deviation. The comparison between cancer tissues and adjacent normal tissues was analyzed by paired *t* test. The comparison between the other two groups was analyzed by unpaired *t* test. Data comparisons among multiple groups were performed using one-way analysis of variance (ANOVA) with Tukey's post hoc test. Cell viability at different time points was analyzed by two-way ANOVA. The correlation between the expression of miR-30d and USP22 and the survival of patients with thyroid cancer was analyzed using Kaplan-Meier analysis and the survival time was analyzed using log-rank method. $p < 0.05$ was considered statistically significant.

Results

miR-30d is poorly expressed in thyroid cancer tissues and associated with the poor prognosis of patients with thyroid cancer

Based on the microarray data (GSE97070) gained from the GEO database, miR-30d was an underexpressed mRNA in thyroid cancer (Fig. 1A). StarBase analysis revealed that the low expression of miR-30d in thyroid cancer was associated with shorter survival time of patients with thyroid cancer (Fig. 1B). Consistent with the results of microarray analysis, miR-30d expression was determined to be much lower in the cancerous tissues of patients with thyroid cancer than in the non-cancerousl tissues by RT-qPCR (Fig. 1C). The survival analysis of patients also revealed that patients with high miR-30d expression had higher 5-year survival rate compared with that of patients with low expression of miR-30d (Fig. 1D). The above results supported that miR-30d was underexpressed in thyroid cancer tissues and its downregulation was associated with poor prognosis of patients with thyroid cancer.

USP22 is negatively regulated by miR-30d

The downstream genes of miR-30d were predicted using the databases mirDIP, microRNA, TargetScan, starBase and DIANA TOOLS, from which 509, 2416, 395, 126 and 1191 downstream genes were obtained, respectively. 17 key genes were obtained from the intersection in Venn diagrams (Fig. 2A). PPI network of these key genes was constructed by String and we observed that PGM3 and GNPDA1 could interact with WDR82 and USP22. USP22 has been identified to play a critical tumor-promotive role in the occurrence of thyroid cancer [10, 11], hence, we selected USP22 as the objective of subsequent experiments. The binding site between miR-30d and USP22 was obtained from microRNA database (Fig. 2B). Dual-luciferase reporter gene assay was conducted to verify their binding, and the results presented that the luciferase activity of USP22-MUT showed no significant change after transfection of miR-30d-mimic ($p > 0.05$), while that of USP22-WT was repressed after transfection of miR-30d-mimic ($p < 0.05$) (Fig. 2C), indicating that miR-30d could specifically bind to USP22. To further identify the regulation of miR-30d on

USP22 expression in thyroid cancer cells, SW579 cells were transfected with miR-30d-mimic. RT-qPCR results revealed that miR-30d expression was upregulated and USP22 mRNA expression was down-regulated in the SW579 cells transfected with miR-30d-mimic (Fig. 2D). Western blot analysis consistently demonstrated that USP22 protein expression was down-regulated by miR-30d (Fig. 2E). The results of RT-qPCR and Western blot analysis additionally presented that USP22 expression was determined to be much higher at mRNA and protein levels in cancerous tissues than in non-cancerous tissues (Fig. 2F & G). The Kaplan-Meier survival analysis also illustrated that the 5-year survival rate of patients with high USP22 expression was much lower than that of patients with low USP22 expression (Fig. 2H). To sum it up, miR-30d downregulated the expression of USP22, and the high expression of USP22 in patients with thyroid cancer was closely related to a poor clinical prognosis.

The promotive effects of miR-30d-mediated USP22 inhibition on the apoptosis of thyroid cancer cells

Considering the deregulation of USP22 in thyroid cancer tissues and its correlation to the clinical prognosis, we further investigated the effect of USP22 on the pathogenesis of thyroid cancer. SW579 cells were transfected with si-USP22 or oe-USP22 and the efficiency of transfection was determined at mRNA and protein levels using RT-qPCR and Western blot analysis (Fig. 3A & B). si-USP22-1, demonstrating the best silencing effect, was selected for subsequent experiments. The data of subsequent CCK8 (Fig. 3C), flow cytometry (Fig. 3D) and TUNEL staining assays (Fig. 3E) illustrated that the viability of SW579 cells was suppressed while cell apoptosis was enhanced in response to USP22 silencing. On the contrary, enhanced cell viability and repressed apoptosis were detected after USP22 overexpression. In addition, the levels of apoptosis-related proteins (Cleaved-caspas-3, caspase-3, Bcl-2 and Bax) were determined by Western blot analysis to further investigate its effect on apoptosis. It was observed that the protein levels of Cleaved-caspas-3 and bax were up-regulated and that of Bcl-2 was down-regulated after USP22 silencing, while USP22 overexpression led to reductions in Cleaved-caspas-3 and Bax along with an elevation in Bcl-2 (Fig. 3F). For the purpose of explaining whether miR-30d-mediated USP22 controlled thyroid cancer cells, the cells were transfected with miR-30d mimic alone, or in combination with oe-USP22. Transfection efficiency was confirmed by RT-qPCR and Western blot analysis. miR-30d mimic transfection led to elevation of miR-30d expression but downregulation of USP22 expression, while the USP22 expression inhibited by miR-30d mimic was restored by co-transfection with oe-USP22 (Fig. 3G). As expected, cell viability was inhibited by enhancement of miR-30d, which was rescued by restoration of USP22 (Fig. 3H). Flow cytometric and TUNEL analyses illustrated that cell apoptosis was promoted by gain-of-function of miR-30d, while this promotion was diminished by restoration of USP22 (Fig. 3I & J). The measurement of pro-apoptotic and anti-apoptotic proteins by Western blot analysis presented the findings that the expression of Cleaved-caspas-3 and Bax was up-regulated at protein levels, and that of Bcl-2 was down-regulated in response to miR-30d mimic transfection. The restoration of USP22 counteracted the effects of miR-30d on the pro-apoptotic and anti-apoptotic proteins mentioned above (Fig. 3K). To conclude, our *in vitro* experiments showed that miR-30d could facilitate the apoptosis of thyroid cancer cells by inhibiting the expression of USP22.

USP22 inhibits the apoptosis of thyroid cancer cells by enhancing the deubiquitination and stability of SIRT1

Above-mentioned results confirmed that miR-30d facilitated the apoptosis of thyroid cancer cells by targeting USP22. Previous literature reported that USP22 can modify the oncogene SIRT1 in thyroid cancer through deubiquitination [14, 21]. Therefore, it was further investigated whether USP22 could deubiquitinate SIRT1 to affect the apoptosis of thyroid cancer cells. SW579 cells were transfected with si-USP22-1 and si-USP22-2, respectively. The results of RT-qPCR and Western blot analysis displayed that the mRNA and protein levels of USP22 and SIRT1 in cells transfected with si-USP22 were significantly lower than that in cells transfected with si-NC (Fig. 4A & B). The sequence with the best silencing effect, si-USP22-1, was selected for subsequent experiments. The binding of USP22 to SIRT1 was detected using Co-IP assay and USP22 was demonstrated to bind to SIRT1 (Fig. 4C). The ubiquitination level of SIRT1 was detected by Western blot analysis, and the results revealed that USP22 silencing substantially promoted the ubiquitination of SIRT1 (Fig. 4D). SW579 cells were treated with CHX and MG132 to test the effect of USP22 on the stability of SIRT1 protein. The protein stability of SIRT1 was impaired as expected after the cells transfected with si-USP22 (Fig. 4E). To test the significance of SIRT1 in thyroid cancer cellular functions, SW579 cells were transfected with si-SIRT1-1 and si-SIRT1-2, and RT-qPCR and Western blot analysis exhibited that the sequence si-SIRT1-1 with the best silencing effect was used in subsequent experiments (Fig. 4F & G). SW579 cells were then transfected with si-SIRT1, or with si-SIRT1 and oe-USP22 in combination. The viability of cells transfected with si-SIRT1 was reduced, but rescued when the cells co-transfected with si-SIRT1 and oe-USP22 (Fig. 4H). Besides, cell apoptosis was promoted by SIRT1 silencing, while this promotion was suppressed by oe-USP22 (Fig. 4I & J). For the molecular characterization, he results of Western blot analysis revealed that the expression of Cleaved-caspas-3, Bax was up-regulated at protein levels and that of Bcl-2 was down-regulated by si-SIRT1 transfection. The co-transfection with oe-USP22 and si-SIRT1 contributed to reductions in Cleaved-caspas-3 and Bax proteins, and increase of Bcl-2 in contrast to transfection with si-SIRT1 (Fig. 4K). In a word, USP22 can suppress apoptosis of thyroid cancer cells by enhancing the stability of SIRT1 through deubiquitination.

SIRT1 inhibits PUMA expression by deacetylating FOXO3a thus further inhibits thyroid cancer cell apoptosis

Recent literature has identified that SIRT1 can deacetylate and modify the transcription factor FOXO3a to control the expression of PUMA [22], which functions as a tumor suppressor gene in the pathogenesis of thyroid cancer through enhancing apoptosis [23]. We herein aimed to determine whether SIRT1 affected the apoptosis of thyroid cancer cells through modulating the acetylation level of FOXO3a and its enrichment in the PUMA promoter. SW579 cells were transfected with si-SIRT1, and its transfection efficiency and its effect on FOXO3a expression were determined by RT-qPCR and Western blot analysis. The expression of FOXO3a was notably elevated at mRNA and protein levels by si-SIRT1 transfection (Fig. 5A & B). The binding of SIRT1 to FOXO3a was detected by Co-IP assay, which revealed that SIRT1 could bind to FOXO3a (Fig. 5C). After SIRT1 silencing, Western blot analysis demonstrated that both the

level of FOXO3a acetylation and its protein level were increased (Fig. 5D). The binding sites between FOXO3a and PUMA promoter region were predicted on the bioinformatic website (http://jaspar.genereg.net) (Fig. 5E). SW579 cells were transfected with oe-FOXO3a and si-FOXO3a, the transfection efficiency was determined by RT-qPCR and Western blot analysis. si-FOXO3a transfection led to reductions in FOXO3a and PUMA at mRNA and protein levels while oe-FOXO3a caused opposite elevations on the contrary (Fig. 5F & G). The binding of FOXO3a to the PUMA promoter region was identified by conducting dual-luciferase report gene assay. The luciferase activity of the PUMA promoter region was enhanced after FOXO3a overexpression (Fig. 5H), indicating that FOXO3a could bind to the PUMA promoter region. Meanwhile, the ChIP assay substantiated the enhanced enrichment of FOXO3a in the promoter region of PUMA in the SW579 cells transfected with oe-FOXO3a (Fig. 5I). For further verification of this regulation mechanism, the expression of PUMA was determined at mRNA and protein levels by RT-qPCR and Western blot analysis by conducting loss- and gain-of-function experiments. The expression of PUMA was up-regulated at mRNA and protein levels in the cells transfected with si-SIRT1, but down-regulated when the cells co-transfected with si-SIRT1 and si-FOXO3a (Fig. 5J). This suggested that SIRT1 downregulated PUMA by positively regulating FOXO3a. In order to investigate whether SIRT1 mediates apoptosis of thyroid cancer cells through FOXO3a-mediated PUMA, SW579 cells were transfected with si-NC, siFOXO3a or co-transfected with si-SIRT1 and si-FOXO3a, the apoptosis of thyroid cancer cells after different transfection was detected by flow cytometry and TUNEL staining. The results showed that cell apoptosis was reduced after transfection of si-FOXO3a, and which was rescued after co-transfection with si-SIRT1 (Fig. 5K & 5L). Taken together, above results supported the finding that SIRT1 could inhibit the expression of PUMA by deacetylation of FOXO3a, thus further impeding the apoptosis of thyroid cancer cells.

miR-30d potentiates apoptosis of thyroid cancer cells by regulating USP22-mediated SIRT1/FOXO3a/PUMA axis

In order to further verify that miR-30d regulates the expression of SIRT1/FOXO3a/PUMA axis through USP22, SW579 cells were co-transfected with miR-30d mimic and oe-USP22/si-SIRT1. RT-qPCR and Western blot analysis showed that the expression of miR-30d, FOXO3a and PUMA was up-regulated while the expression of USP22 and SIRT1 was down-regulated in cells transfected with miR-30d mimic. miR-30d, USP22 and SIRT1 were elevated and FOXO3a and PUMA were reduced in cells co-transfected with miR-30d mimic and oe-USP22. miR-30d, FOXO3a and PUMA were increased while USP22 and SIRT1 were decreased in cells co-transfected with miR-30d mimic and si-SIRT1 (Fig. 6A & B). The results of flow cytometry and TUNEL staining exhibited that compared with that of cells co-transfected with miR-30d mimic and oe-NC, apoptosis rate of cells co-transfected with miR-30d mimic and oe-USP22 was repressed, and that of cells co-transfected with miR-30d mimic and si-SIRT1 was elevated (Fig. 6C & D). In short, miR-30d can inhibit the apoptosis of thyroid cancer cells by regulating the SIRT1/FOXO3a/PUMA axis through USP22.

miR-30d retards tumorigenicity of thyroid cancer cells through USP22 inhibition

In vivo experiments were conducted accordingly that xenograft tumors were transplanted into nude mouse subcutaneously. SW579 cells stably infected with lentivirus expressing miR-30d mimic and oe-USP22/miR-30d mimic and their negative controls (mimic-NC, oe-NC) were injected into the axilla of mice. The tumor volume and weight were much lowered by the enhancement of miR-30d in the tumor-bearing mice. In the meanwhile, the tumor volume and weight were markedly increased by overexpression of USP22 in the presence of miR-30d (Fig. 7A - C). HE staining of the tumor tissues uncovered that the degree of tumor tissue lesions could be decreased by miR-30d, but increased by restoration of USP22 (Fig. 7D). TUNEL staining displayed that cell apoptosis in tumor tissues was elevated by miR-30d, but this elevation was diminished by restoration of USP22 (Fig. 7E). As seen from the results of RT-qPCR and Western blot analyses, USP22 and SIRT1 were reduced notably and FOXO3a and PUMA were increased remarkably at mRNA and protein levels in response to enhancement of miR-30d. SIRT1 was sharply elevated while FOXO3a and PUMA were reduced at mRNA and protein levels by restoration of USP22 (Fig. 7F & G). Furthermore, the levels of apoptosis-related proteins Cleaved-caspas-3, caspase-3, Bcl-2 and Bax were determined by Western blot analysis. The results revealed that Bcl-2 protein level was reduced, and the levels of Cleaved-caspas-3 and Bax proteins were increased after miR-30d gain-of-function. On the contrary, the changes in the pro-apoptotic and anti-apoptotic proteins induced by miR-30d mimic could be counteracted by oe-USP22 simultaneously (Fig. 7G). Above results supported that miR-30d could negatively regulate USP22 to suppress the thyroid tumorigenesis *in vivo*.

Discussion

Increasing attention has come to be attracted on the function of miRNAs as important biomarkers or mediators underlying the tumorigenesis of thyroid [24, 25]. The current study mainly addressed the specific functions of miR-30d and molecular mechanisms by which miR-30d involved in the development of thyroid cancer, and our results presented that miR-30d could promote cell apoptosis through mediating USP22/SIRT1/FOXO3a/PUMA axis, thereby slowing down thyroid tumorigenesis ultimately (Fig. 8).

The initial findings in the current study were that miR-30d was poorly expressed in human thyroid cancer tissues and the low expression of miR-30d was associated with the poor prognosis of patients with thyroid cancer. The dysregulation of miR-30d and its important role have been shown in other human cancers, especially gastrointestinal malignancies. Likewise, it was identified that miR-30d was down-regulated in both cells and tissues of NSCLC and its expression shared an association with clinicopathological features [26]. miR-30d was evidenced as a tumor-suppressive miRNA in esophageal squamous cell carcinoma [27]. Downregulation of miR-30d correlated with aggressive cancer progression while its ectopic expression contributed to suppression of cancer development in colorectal carcinoma [28]. miR-30d functioned as a tumor suppressor by facilitating cancer cell apoptosis [29]. Partially consistent with our finding, miR-30d was determined to be one of down-regulated miRNA in ATC, the least

common but the most fatal thyroid cancer [30]. The down-regulation and anti-tumor effect of miR-30d have been addressed on ATC [31]. Our study provided main evidence for the pro-apoptotic effect of miR-30d on thyroid cancer cells which was also supported by increases in Cleaved-caspas-3, caspase-3 and Bax and reduction in Bcl-2. Cleaved-caspas-3, caspase-3, Bax and Bcl-2 are all known apoptosis-related proteins with Bcl-2 functioning as an antiapoptotic protein and the rest three as pro-apoptotic proteins [32, 33]. Further, USP22 was observed to be regulated by miR-30d and USP22 inhibition was responsible for the promoted apoptosis of thyroid cancer cells by miR-30d. USP22 knockdown was observed to promote apoptosis of ATC cells by upregulating Bax and Bid and activating caspase-3 [11]. A previous study revealed that USP22 was abnormally highly expressed in thyroid cancer tissues and its high expression was related to the poor prognosis of patients with thyroid cancer [10]. Moreover, it was also identified that USP22 can be regulated by miR-101 negatively and USP22 knockdown were identified as depressors of thyroid cancer growth and metastasis [12]. In combination with the *in vivo* data, our findings supported the anti-tumor effect of miR-30d by inhibiting USP22.

We further demonstrated that USP22 restrained thyroid cancer cell apoptosis by enhancing SIRT1 deubiquitination, and SIRT1 could also decrease cell apoptosis through FOXO3a deacetylation-induced PUMA repression. SIRT1 is an NAD(+)-dependent histone deacetylase and implicated in several biological processes such as senescence, stress reaction and cell survival [34]. SIRT1 deubiquitination is crucial to its function in cell apoptosis and survival in response to DNA damage [35, 36]. Consistent with our finding, SIRT1 was also confirmed as an oncogene for thyroid cancer [37]. SIRT1 was also positively regulated by USP22 and USP22 further promotes multidrug resistance of hepatocellular carcinoma cells by activating SIRT1 [21]. FOXO3a is a tumor suppressor belonging to the forkhead transcription factor O subfamily [38]. It was reported that SIRT1 was able to deacetylate various substrates including FOXO3a, thereby decreasing the expression of FOXO3a [39, 40], which was substantiated in this study. In addition to this finding, our study further demonstrated this interaction in the regulation of thyroid cancer cell apoptosis. In the meantime, this interaction was found to be involved in the pathogenesis of autoimmune thyroid diseases [17]. Sun et al also validated that the elevation of PUMA induced by FOXO3a exerted a repressing effect in the development of colon cancer [41]. Furthermore, a previous research has demonstrated PUMA up-regulation as a contributor of antitumor activity in ATC [42]. Therefore, it was safe to conclude that USP22 played a suppressive role in the apoptosis of thyroid cancer cells through mediating SIRT1/FOXO3a/PUMA axis.

Conclusion

Taken together, this study supported the pro-apoptotic and an-tumor effects of miR-30d on thyroid cancer cells. The modulatory axis USP22/SIRT1/FOXO3a/PUMA proposed in our study can assist in better acknowledgement of the anti-tumor mechanisms. However, the underlying interaction of miRNAs in thyroid cancer needs more excavation, which might provide novel potential targets for effective management for thyroid diseases. In spite of that, this study validated the tumor-suppressing effect of miR-30d, which may be a promising clinically viable target in thyroid cancer treatment if the findings could be substantiated in clinical setting in the future experiments.

Abbreviations

miRNAs (MicroRNAs); USP22 (ubiquitin-specific protease 22); PTC (papillary thyroid cancer); FTC (follicular thyroid cancer); MTC (medullary thyroid cancer); ATC (anaplastic thyroid cancer); SIRT1 (sirtuin-1); FoxO3a (factor O3a); PUMA (P53-up-regulated modulator of apoptosis); GEO (Gene Expression Omnibus); PPI (protein-protein-interaction); ATCC (American Type Culture Collection); NC (negative control); MUT (mutation); WT (wild type).

Declarations

Availability of data and materials
The authors confirm that the data supporting the findings of this study are available within the article.

Ethics approval and consent to participate
The current study was performed with the approval of the Ethics Committee of the First Affiliated Hospital of Xi'an Jiaotong University and the procedures conformed to the Declaration of Helsinki. Written informed consent was obtained from each participant. Animal experimental procedures were in strict accordance with recommendations in the Guide for the Care and Use of Laboratory Animals issued by the National Institutes of Health.

Consent for publication
Not applicable.

Authors' contributions

Yuan Shao, Shaoqiang Zhang and Xiaoxia Wang wrote the paper; Xin Sun, Jie Wu and Fang Sui conceived the experiments; Fangli Yang, Hao Dai, Junsong Liu and XiaoBao Yao analyzed the data; Honghui Li, Lifeng Liu , Xuan Wang , Zhiwei Zheng , and Chongwen Xu collected and provided the sample for this study. All authors have read and approved the final submitted manuscript.

Competing interests

The authors declare that they have no competing interests.

References

1. Lin JD, Liou MJ, Hsu HL, Leong KK, Chen YT, Wang YR, et al. Circulating Epithelial Cell Characterization and Correlation with Remission and Survival in Patients with Thyroid Cancer. Thyroid. 2018;28:1479–89.

2. Bray F, Ferlay J, Soerjomataram I, Siegel RL, Torre LA, Jemal A. Global cancer statistics 2018: GLOBOCAN estimates of incidence and mortality worldwide for 36 cancers in 185 countries. CA Cancer J Clin. 2018;68:394–424.

3. Jin J. JAMA patient page. Screening for Thyroid Cancer. JAMA. 2017; 317:1920.

4. Raue F, Frank-Raue K. Thyroid Cancer: Risk-Stratified Management and Individualized Therapy. Clin Cancer Res. 2016;22:5012–21.

5. Filetti S, Durante C, Hartl D, Leboulleux S, Locati LD, Newbold K, et al. Thyroid cancer: ESMO Clinical Practice Guidelines for diagnosis, treatment and follow-updagger. Ann Oncol. 2019;30:1856–83.

6. Xu X, Long H, Xi B, Ji B, Li Z, Dang Y, et al. Molecular Network-Based Drug Prediction in Thyroid Cancer. Int J Mol Sci. 2019; 20.

7. Fuziwara CS, Kimura ET. MicroRNAs in thyroid development, function and tumorigenesis. Mol Cell Endocrinol. 2017;456:44–50.

8. Pallante P, Battista S, Pierantoni GM, Fusco A. Deregulation of microRNA expression in thyroid neoplasias. Nat Rev Endocrinol. 2014;10:88–101.

9. Zhang Y, Yang WQ, Zhu H, Qian YY, Zhou L, Ren YJ, et al. Regulation of autophagy by miR-30d impacts sensitivity of anaplastic thyroid carcinoma to cisplatin. Biochem Pharmacol. 2014;87:562–70.

10. Wang H, Li YP, Chen JH, Yuan SF, Wang L, Zhang JL, et al. Prognostic significance of USP22 as an oncogene in papillary thyroid carcinoma. Tumour Biol. 2013;34:1635–9.

11. Zhao HD, Tang HL, Liu NN, Zhao YL, Liu QQ, Zhu XS, et al. Targeting ubiquitin-specific protease 22 suppresses growth and metastasis of anaplastic thyroid carcinoma. Oncotarget. 2016;7:31191–203.

12. Zhao H, Tang H, Huang Q, Qiu B, Liu X, Fan D, et al. MiR-101 targets USP22 to inhibit the tumorigenesis of papillary thyroid carcinoma. Am J Cancer Res. 2016;6:2575–86.

13. Wu W, Zhang L, Lin J, Huang H, Shi B, Lin X, et al. Hypermethylation of the HIC1 promoter and aberrant expression of HIC1/SIRT1 contribute to the development of thyroid papillary carcinoma. Oncotarget. 2016;7:84416–27.

14. Herranz D, Maraver A, Canamero M, Gomez-Lopez G, Inglada-Perez L, Robledo M, et al. SIRT1 promotes thyroid carcinogenesis driven by PTEN deficiency. Oncogene. 2013;32:4052–6.

15. Xu G, Cai J, Wang L, Jiang L, Huang J, Hu R, et al. MicroRNA-30e-5p suppresses non-small cell lung cancer tumorigenesis by regulating USP22-mediated Sirt1/JAK/STAT3 signaling. Exp Cell Res. 2018;362:268–78.

16. Marlow LA, von Roemeling CA, Cooper SJ, Zhang Y, Rohl SD, Arora S, et al. Foxo3a drives proliferation in anaplastic thyroid carcinoma through transcriptional regulation of cyclin A1: a paradigm shift that impacts current therapeutic strategies. J Cell Sci. 2012;125:4253–63.

17. Roehlen N, Doering C, Hansmann ML, Gruenwald F, Vorlaender C, Bechstein WO, et al. Vitamin D, FOXO3a, and Sirtuin1 in Hashimoto's Thyroiditis and Differentiated Thyroid Cancer. Front Endocrinol (Lausanne). 2018;9:527.

18. Yang J, Zhao X, Tang M, Li L, Lei Y, Cheng P, et al. The role of ROS and subsequent DNA-damage response in PUMA-induced apoptosis of ovarian cancer cells. Oncotarget. 2017;8:23492–506.

19. Panda PK, Naik PP, Meher BR, Das DN, Mukhopadhyay S, Praharaj PP, et al. PUMA dependent mitophagy by Abrus agglutinin contributes to apoptosis through ceramide generation. Biochim Biophys Acta Mol Cell Res. 2018;1865:480–95.

20. Dey P, Strom A, Gustafsson JA. Estrogen receptor beta upregulates FOXO3a and causes induction of apoptosis through PUMA in prostate cancer. Oncogene. 2014;33:4213–25.

21. Ling S, Li J, Shan Q, Dai H, Lu D, Wen X, et al. USP22 mediates the multidrug resistance of hepatocellular carcinoma via the SIRT1/AKT/MRP1 signaling pathway. Mol Oncol. 2017;11:682–95.

22. Zhao X, Liu Y, Zhu G, Liang Y, Liu B, Wu Y, et al. SIRT1 downregulation mediated Manganese-induced neuronal apoptosis through activation of FOXO3a-Bim/PUMA axis. Sci Total Environ. 2019;646:1047–55.

23. Yin Q, Liu S, Dong A, Mi X, Hao F, Zhang K. Targeting Transforming Growth Factor-Beta1 (TGF-beta1) Inhibits Tumorigenesis of Anaplastic Thyroid Carcinoma Cells Through ERK1/2-NFkappakB-PUMA Signaling. Med Sci Monit. 2016;22:2267–77.

24. Rosignolo F, Memeo L, Monzani F, Colarossi C, Pecce V, Verrienti A, et al. MicroRNA-based molecular classification of papillary thyroid carcinoma. Int J Oncol. 2017;50:1767–77.

25. Zhang Y, Pan J, Xu D, Yang Z, Sun J, Sun L, et al. Combination of serum microRNAs and ultrasound profile as predictive biomarkers of diagnosis and prognosis for papillary thyroid microcarcinoma. Oncol Rep. 2018;40:3611–24.

26. Wu Y, Zhang J, Hou S, Cheng Z, Yuan M. Non-small cell lung cancer: miR-30d suppresses tumor invasion and migration by directly targeting NFIB. Biotechnol Lett. 2017;39:1827–34.

27. Xie R, Wu SN, Gao CC, Yang XZ, Wang HG, Zhang JL, et al. MicroRNA-30d inhibits the migration and invasion of human esophageal squamous cell carcinoma cells via the posttranscriptional regulation of enhancer of zeste homolog 2. Oncol Rep. 2017;37:1682–90.

28. Yan L, Qiu J, Yao J. Downregulation of microRNA-30d promotes cell proliferation and invasion by targeting LRH-1 in colorectal carcinoma. Int J Mol Med. 2017;39:1371–80.

29. Zhang R, Xu J, Zhao J, Bai J. Mir-30d suppresses cell proliferation of colon cancer cells by inhibiting cell autophagy and promoting cell apoptosis. Tumour Biol. 2017;39:1010428317703984.

30. Visone R, Pallante P, Vecchione A, Cirombella R, Ferracin M, Ferraro A, et al. Specific microRNAs are downregulated in human thyroid anaplastic carcinomas. Oncogene. 2007;26:7590–5.

31. Esposito F, Tornincasa M, Pallante P, Federico A, Borbone E, Pierantoni GM, et al. Down-regulation of the miR-25 and miR-30d contributes to the development of anaplastic thyroid carcinoma targeting the polycomb protein EZH2. J Clin Endocrinol Metab. 2012;97:E710-8.

32. Natalino RJ, Antoneli CB, Ribeiro KC, Campos AH, Soares FA. Immunohistochemistry of apoptosis-related proteins in retinoblastoma. Pathol Res Pract. 2016;212:1144–50.

33. Qiu XG, Chen YD, Yuan J, Zhang N, Lei T, Liu J, et al. Functional BCL-2 rs2279115 Promoter Noncoding Variant Contributes to Glioma Predisposition, Especially in Males. DNA Cell Biol. 2019;38:85–90.

34. Koga T, Suico MA, Shimasaki S, Watanabe E, Kai Y, Koyama K, et al. Endoplasmic Reticulum (ER) Stress Induces Sirtuin 1 (SIRT1) Expression via the PI3K-Akt-GSK3beta Signaling Pathway and Promotes Hepatocellular Injury. J Biol Chem. 2015;290:30366–74.

35. Liang Q, Dexheimer TS, Zhang P, Rosenthal AS, Villamil MA, You C, et al. A selective USP1-UAF1 inhibitor links deubiquitination to DNA damage responses. Nat Chem Biol. 2014;10:298–304.

36. Peng L, Yuan Z, Li Y, Ling H, Izumi V, Fang B, et al. Ubiquitinated sirtuin 1 (SIRT1) function is modulated during DNA damage-induced cell death and survival. J Biol Chem. 2015;290:8904–12.

37. Li D, Bai L, Wang T, Xie Q, Chen M, Fu Y, et al. Function of miR-212 as a tumor suppressor in thyroid cancer by targeting SIRT1. Oncol Rep. 2018;39:695–702.

38. Li X, Liu K, Zhou W, Jiang Z. MiR-155 targeting FoxO3a regulates oral cancer cell proliferation, apoptosis, and DDP resistance through targeting FoxO3a. Cancer Biomark. 2020;27:105–11.

39. Wang YQ, Cao Q, Wang F, Huang LY, Sang TT, Liu F, et al. SIRT1 Protects Against Oxidative Stress-Induced Endothelial Progenitor Cells Apoptosis by Inhibiting FOXO3a via FOXO3a Ubiquitination and Degradation. J Cell Physiol. 2015;230:2098–107.

40. An BS, Tavera-Mendoza LE, Dimitrov V, Wang X, Calderon MR, Wang HJ, et al. Stimulation of Sirt1-regulated FoxO protein function by the ligand-bound vitamin D receptor. Mol Cell Biol. 2010;30:4890–900.

41. Sun L, Huang Y, Liu Y, Zhao Y, He X, Zhang L, et al. Ipatasertib, a novel Akt inhibitor, induces transcription factor FoxO3a and NF-kappaB directly regulates PUMA-dependent apoptosis. Cell Death Dis. 2018;9:911.

42. Pan Y, Liu P, Chen D, Dou L. Small interfering RNA (siRNA) against Slug induces apoptosis and sensitizes human anaplastic thyroid carcinoma cells to doxorubicin. Cancer Biomark. 2017;18:357–66.
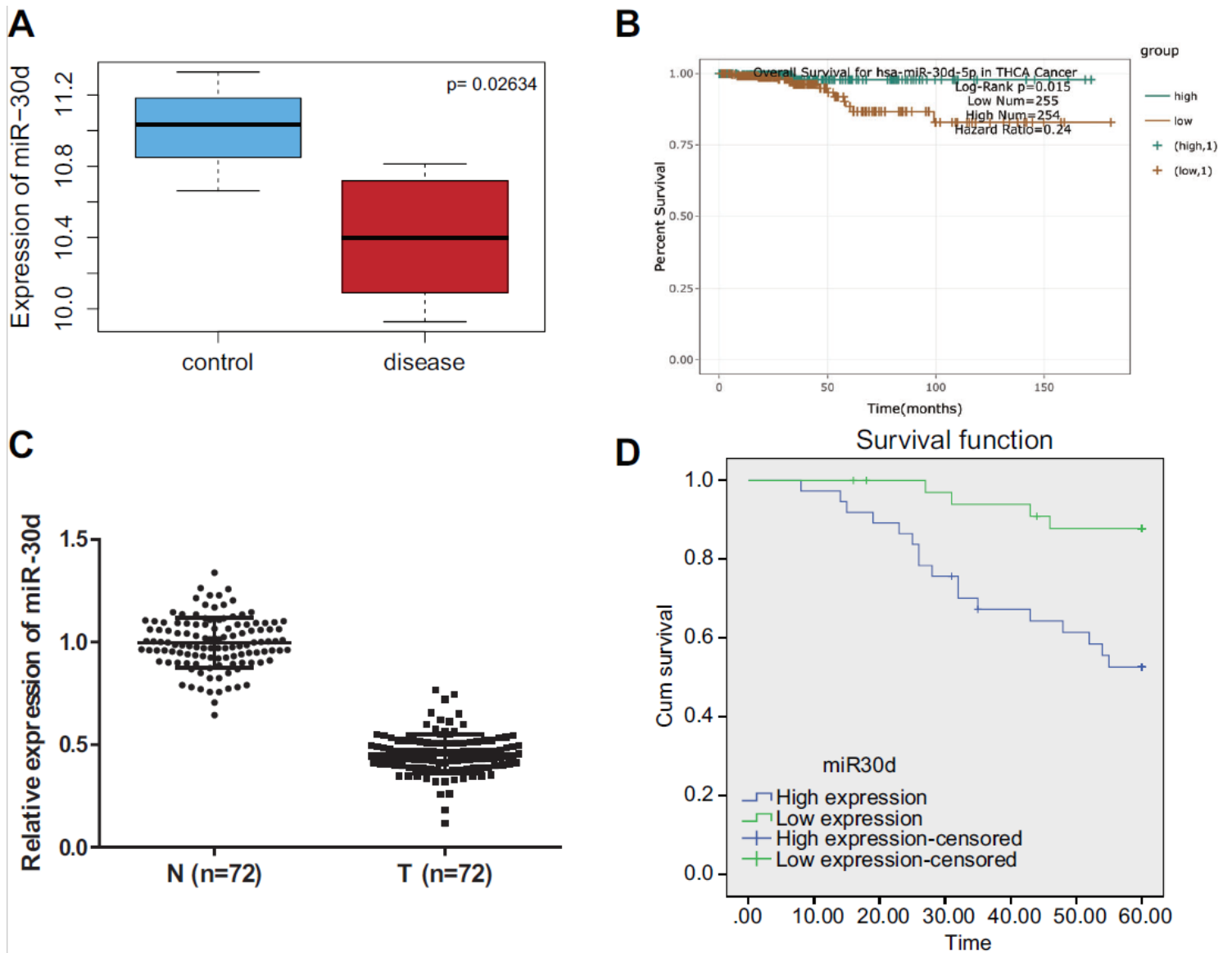
Figures

Figure 1

The low expression of miR-30d in thyroid cancer tissues was associated with the poor prognosis of patients with thyroid cancer. A, Box plot of miR-30d expression in thyroid cancer (red box on the right) and non-neoplastic thyroid (blue box on the left) samples according to GSE97070 microarray. B, The correlation between the survival of patients with thyroid cancer and the expression of miR-30d obtained by starBase analysis. Survival curve (HR = 0.24, P = 0.015). C, The expression of miR-30d in thyroid cancer tissues and non-cancerous tissues (n = 72) determined by RT-qPCR. D, The correlation analysis between miR-30d expression in patients with thyroid cancer and patient survival time. * p < 0.05 compared with non-cancerous samples. The experiment was repeated three times. Data analysis between cancerous tissues and non-cancerous tissues was performed using paired t-test, Kaplan-Meier survival analysis was performed to explore the relationship between miR-30d expression and survival rate of patients with thyroid cancer.
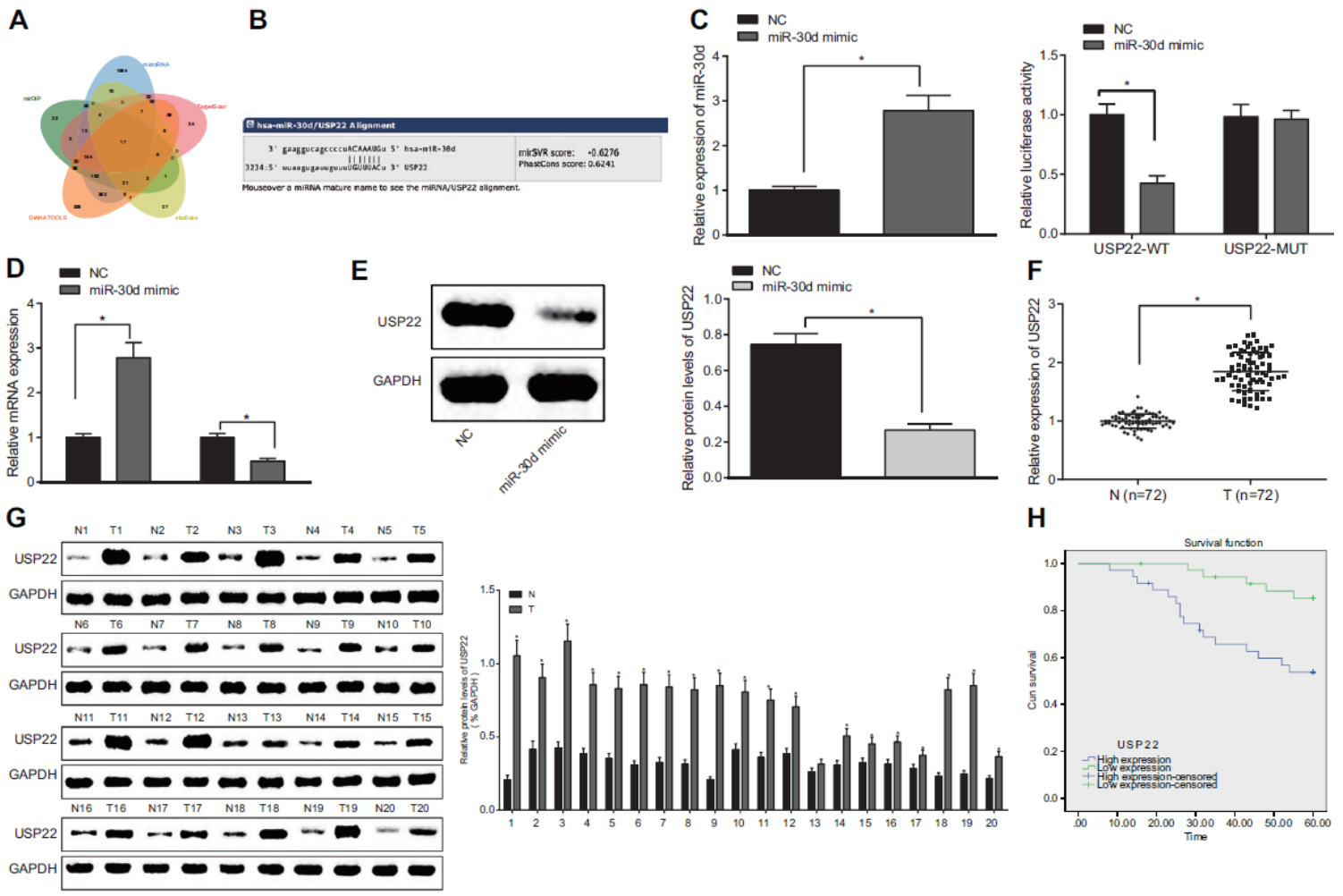
Figure 2

miR-30d negatively regulated the expression of USP22. A, Venn map of the downstream genes of miR-30d predicted by the databases mirDIP, microRNA, TargetScan, starBase, and DIANA TOOLS, with 17 intersecting genes. B, The binding sites of miR-30d on the 3'UTR of USP22 predicted by microRNA database. C, The transfection efficiency of miR-30d mimic determined by RT-qPCR and the binding of miR-30d to USP22 determined by dual-luciferase reporter gene assay. D, The expression of miR-30d and USP22 in cells transfected with miR-30d mimic determined by RT-qPCR. E, USP22 protein level in cells transfected with miR-30d mimic determined by Western blot analysis. F, The expression of USP22 mRNA in thyroid cancer tissues and non-cancerous tissues (n = 72) determined by RT-qPCR. G, The expression of USP22 protein thyroid cancer tissues and non-cancerous tissues (n = 72) determined by Western blot analysis. H, The correlation analysis between the expression of USP22 in thyroid cancer patients and patient survival. * p < 0.05. The experiment was repeated 3 times. The paired t-test was used to analyze the data between the cancer tissues and non-cancerous tissues. The data between the other two groups were analyzed by unpaired t-test. The correlation between USP22 expression and the survival rate of patients with thyroid cancer was analyzed by Kaplan-Meier analysis.
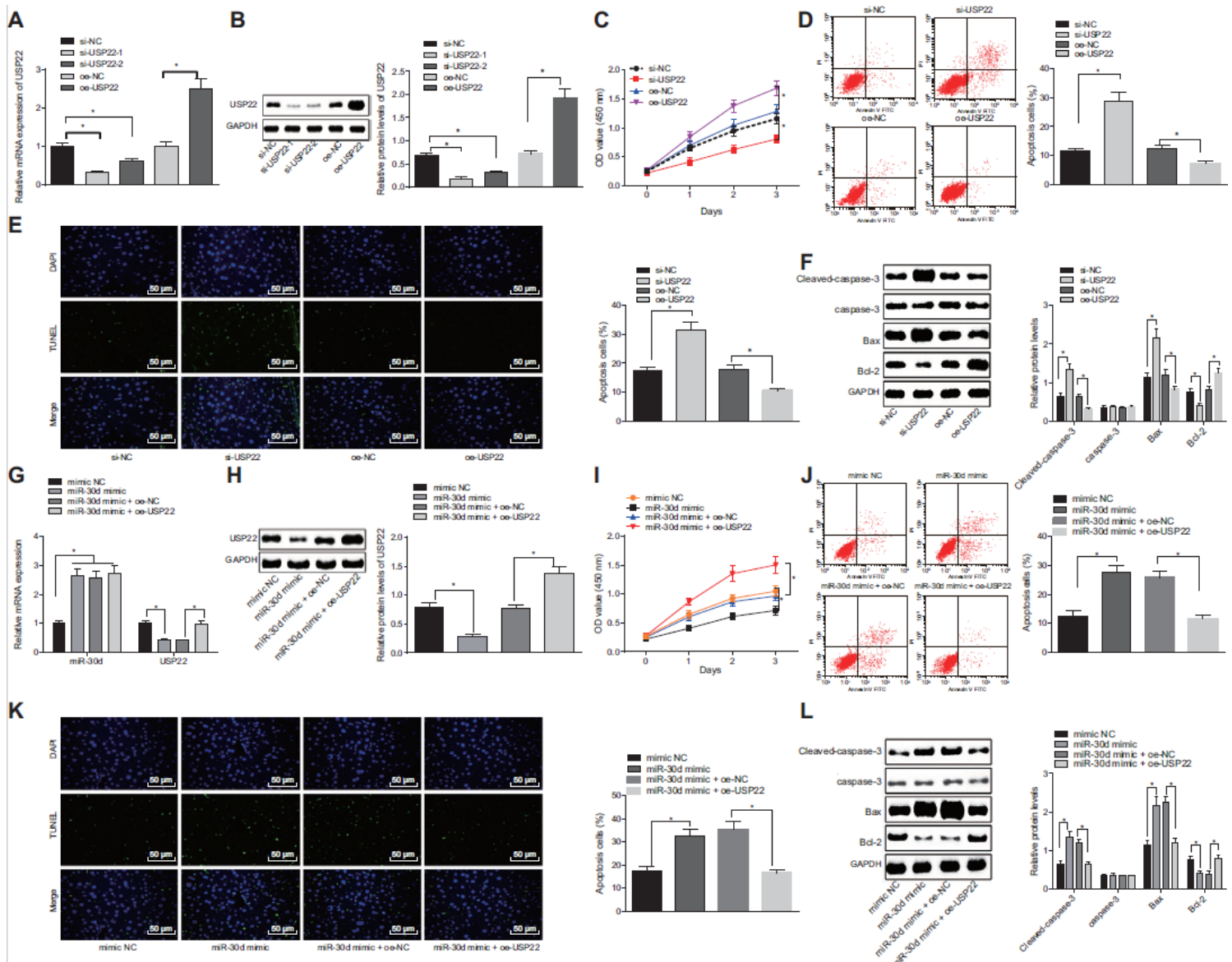
Figure 3

miR-30d reduces the expression of USP22 and thus further promotes cell apoptosis. A and B, The transfection efficiency of si-USP22 and oe-USP22 in SW579 cells for silencing and overexpression determined at mRNA level by RT-qPCR (A) and at protein level by Western blot analysis (B). C, The OD value for SW579 cell viability after USP22 silencing and overexpression detected by CCK8 assay. D, Cell apoptosis after USP22 silencing and overexpression in SW579 cells detected by flow cytometry. E, Cell apoptosis after USP22 silencing and overexpression in SW579 cells detected by TUNEL staining (× 100). F, The expression of apoptosis-related proteins (Cleaved-caspas-3, caspase-3. Bcl-2 and Bax) responding to USP22 silencing and overexpression determined by Western blot analysis. G, Transfection efficiency of miR-30d mimic and oe-USP22 determined at mRNA and protein levels by RT-qPCR and Western blot analysis. H, Cell viability after miR-30d and/or USP22 overexpression detected by CCK8 assay. I, Cell apoptosis after miR-30d and/or USP22 overexpression detected by flow cytometry. J, Cell apoptosis after miR-30d and/or USP22 overexpression detected by TUNEL staining (× 100). K, The expression of apoptosis-related proteins (Cleaved-caspas-3, caspase-3, Bcl-2 and Bax) after overexpression of miR-30d

and/or USP22 determined by Western blot analysis. * p < 0.05. The experiment was repeated 3 times. Unpaired t-test was used for comparison between two groups. One-way ANOVA was used for data analysis among multiple groups. Two-way ANOVA was used for data analysis among multiple groups at different time points.
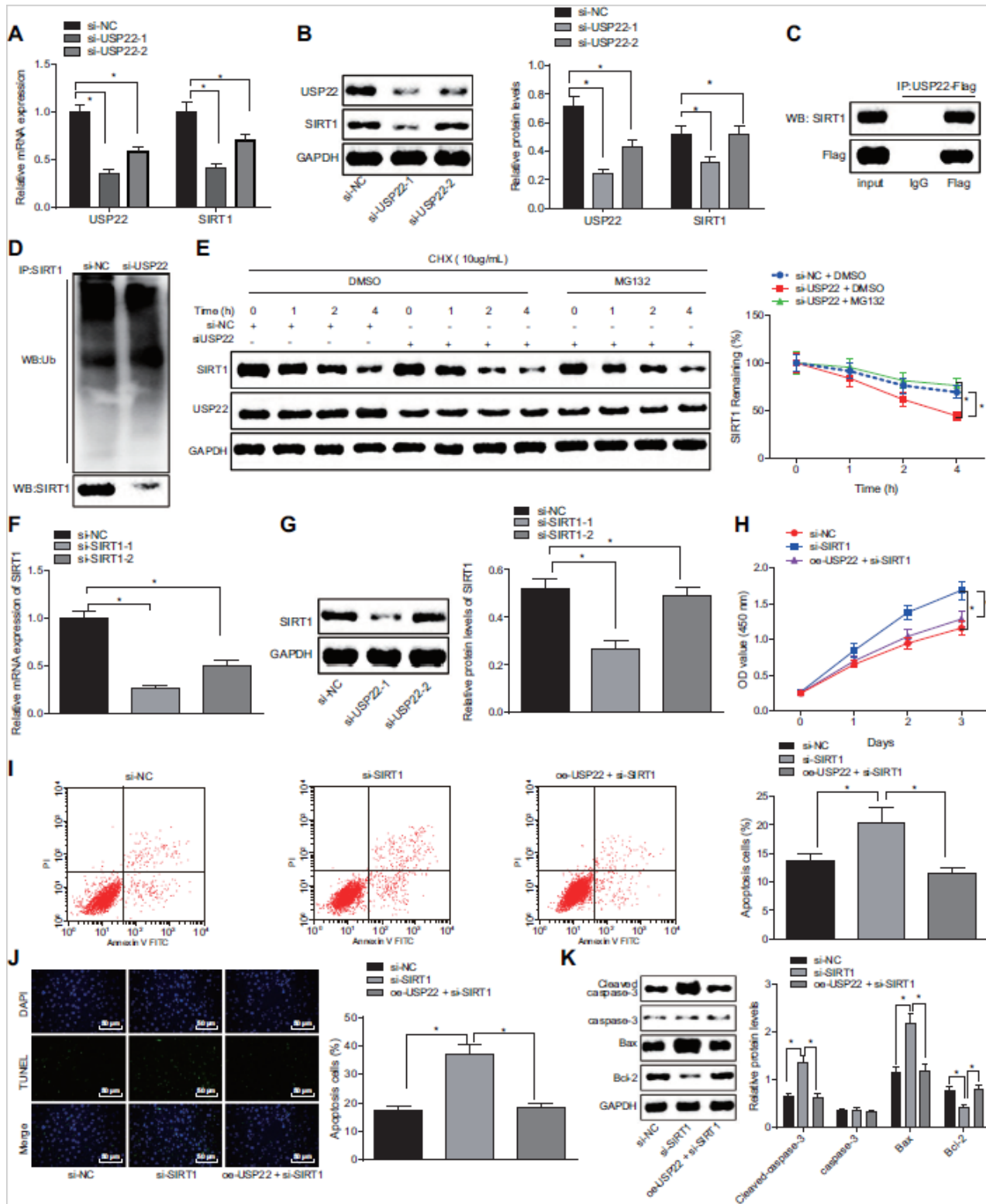

Figure 4

The stability of SIRT1 were enhanced by USP22 through deubiquitination, inhibiting the apoptosis of thyroid cancer cells. A, The silencing efficiency of si-USP22 and the mRNA level of SIRT1 after si-USP22 transfection determined by RT-qPCR. B, The silencing efficiency of si-USP22 and the protein level of SIRT1 after si-USP22 transfection determined by Western blot analysis. C, The binding of USP22 to SIRT1 detected by Co-IP. D, The ubiquitination level of SIRT1 in SW579 cells transfected with si-USP22 determined by Western blot analysis. E, The protein degradation of SIRT1 in SW579 cells transfected with si-USP22 determined by Western blot analysis after treatment with CHX and MG132. F, The silencing efficiency of si-SIRT1 determined at mRNA level by RT-qPCR. G, The silencing efficiency of si-SIRT1 determined at protein level by Western blot analysis. H, Cell viability after SIRT1 silencing alone or USP22 overexpression in combination detected by CCK8. I, Cell apoptosis after SIRT1 silencing alone or USP22 overexpression in combination detected by flow cytometry. J, Cell apoptosis after SIRT1 silencing alone or USP22 overexpression in combination detected by TUNEL staining (× 200). K, The expression of apoptosis-related proteins (Cleaved-caspas-3, caspase-3, Bcl-2, and bax) after SIRT1 silencing alone or USP22 overexpression in combination determined by Western blot analysis, * p < 0.05. The experiment was repeated 3 times, and the analysis of data between multiple groups was performed by one-way ANOVA. Comparison of multiple groups at different time points was performed using two-way ANOVA.
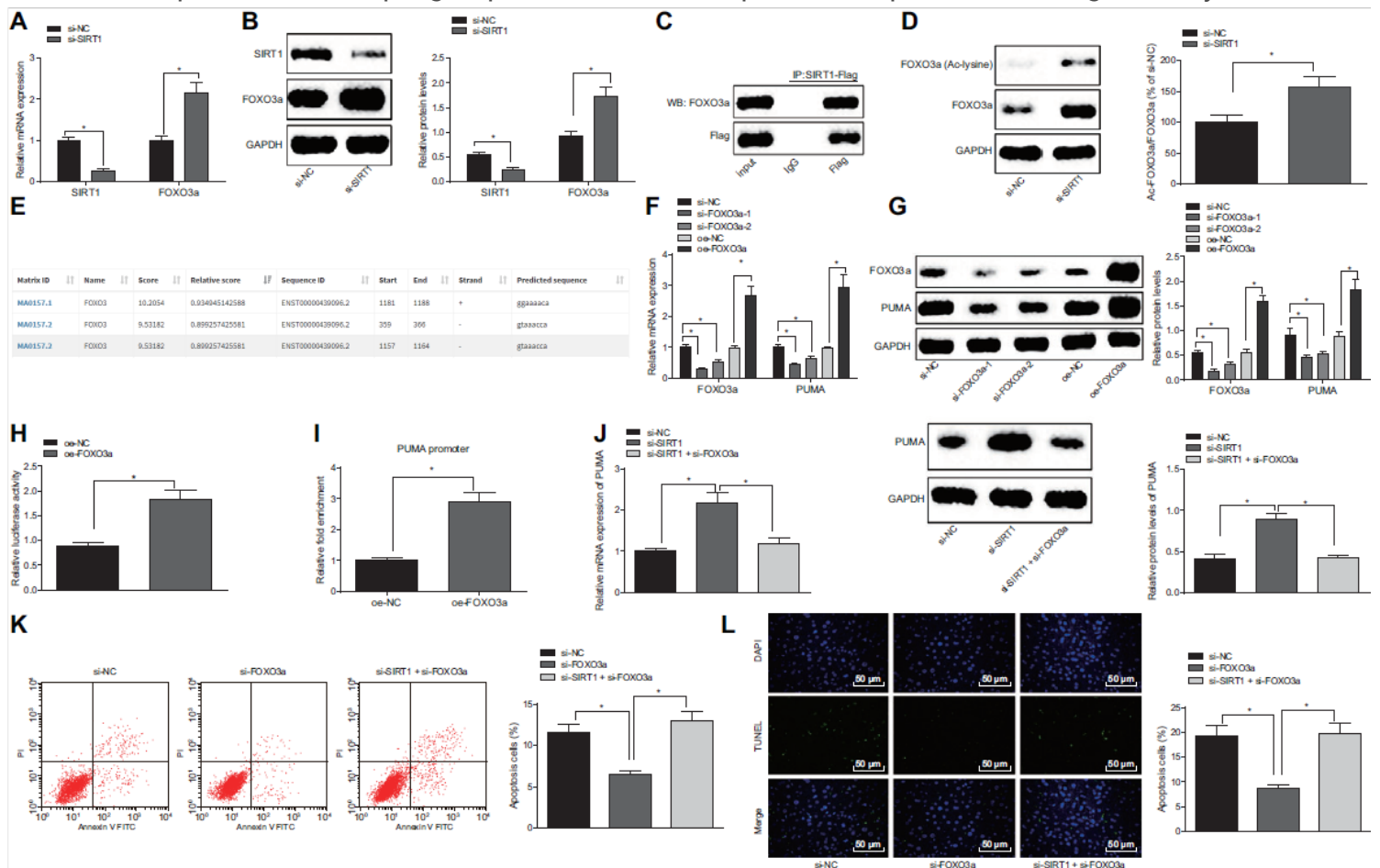

Figure 5

Thyroid cancer cell apoptosis was inhibited by SIRT1 through PUMA inhibition induced by FOXO3a deacetylation. A, The mRNA expression of SIRT1 and FOXO3a after SW579 cells were transfected with si-SIRT1 determined by RT-qPCR. B, The protein expression of SIRT1 and FOXO3a after SW579 cells were transfected with si-SIRT1 determined by Western blot analysis. C, The binding of SIRT1 to FOXO3a detected by Co-IP assay. D, The acetylation level of FOXO3a after SIRT1 silencing determined by Western blot analysis. E, The predicted binding site between FOXO3a and PUMA promoter region by JASPAR database. F, The mRNA expression of FOXO3a and PUMA after SW579 cells were transfected with si-FOXO3a or oe-FOXO3a determined by RT-qPCR. G, The protein expression of FOXO3a and PUMA after SW579 cells were transfected with si-FOXO3a or oe-FOXO3a determined by Western blot analysis. H, The binding of FOXO3a to the PUMA promoter region identified by dual-luciferase report gene assay. I, The enrichment of FOXO3a in the PUMA promoter region after FOXO3a overexpression determined by ChIP assay. J, The mRNA and protein levels of PUMA in SW579 cells transfected with si-NC/si-SIRT1 or co-transfected with si-SIRT1 and si-FOXO3a determined by RT-qPCR and Western blot analysis, respectively. K, Cell apoptosis after SIRT1 and FOXO3a silencing detected by flow cytometry. L, Cell apoptosis after SIRT1 and FOXO3a silencing detected by TUNEL staining (× 200). * $p < 0.05$. The experiment was repeated 3 times. Unpaired t-test was used for comparison between two groups. One-way ANOVA was used for data analysis among multiple groups.
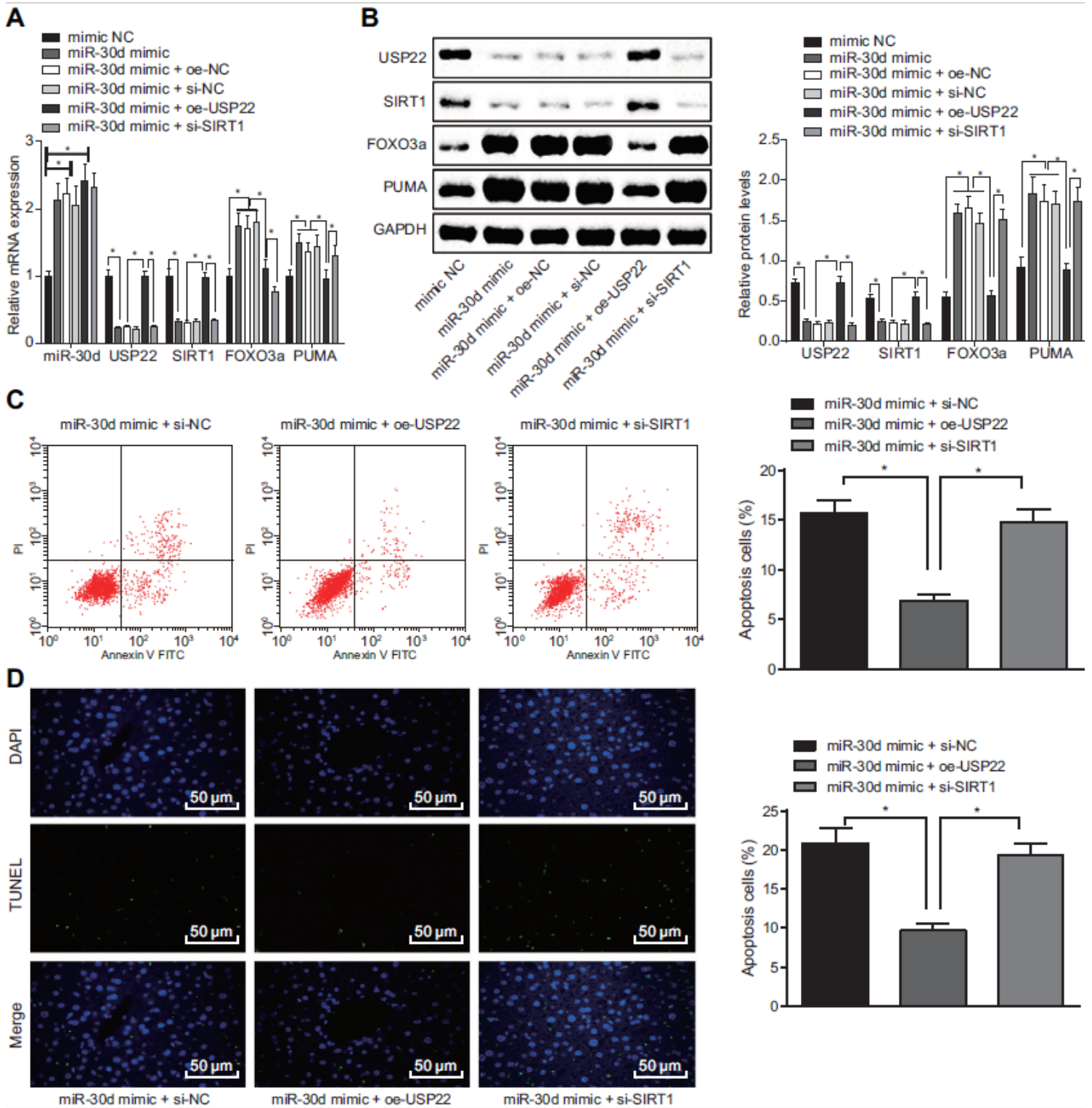
Figure 6

miR-30d mediates the SIRT1/FOXO3a/PUMA axis by inhibiting USP22, thereby facilitating apoptosis of thyroid cancer cells. A, The expression of miR-30d, and mRNA levels of USP22, SIRT1, FOXO3a and PUMA after co-transfection with miR-30d mimic and oe-USP22/si-SIRT1 determined by RT-qPCR. B, The protein levels of USP22, SIRT1, FOXO3a and PUMA after co-transfection with miR-30d mimic and oe-USP22/si-SIRT1 determined by Western blot analysis. C, Cell apoptosis after o-transfection with miR-30d mimic and

oe-USP22/si-SIRT1 detected by flow cytometry. D, Cell apoptosis after o-transfection with miR-30d mimic and oe-USP22/si-SIRT1 detected by TUNEL staining (× 200). * p < 0.05. The experiment was repeated 3 times, and the analysis of data among multiple groups was performed by one-way ANOVA.
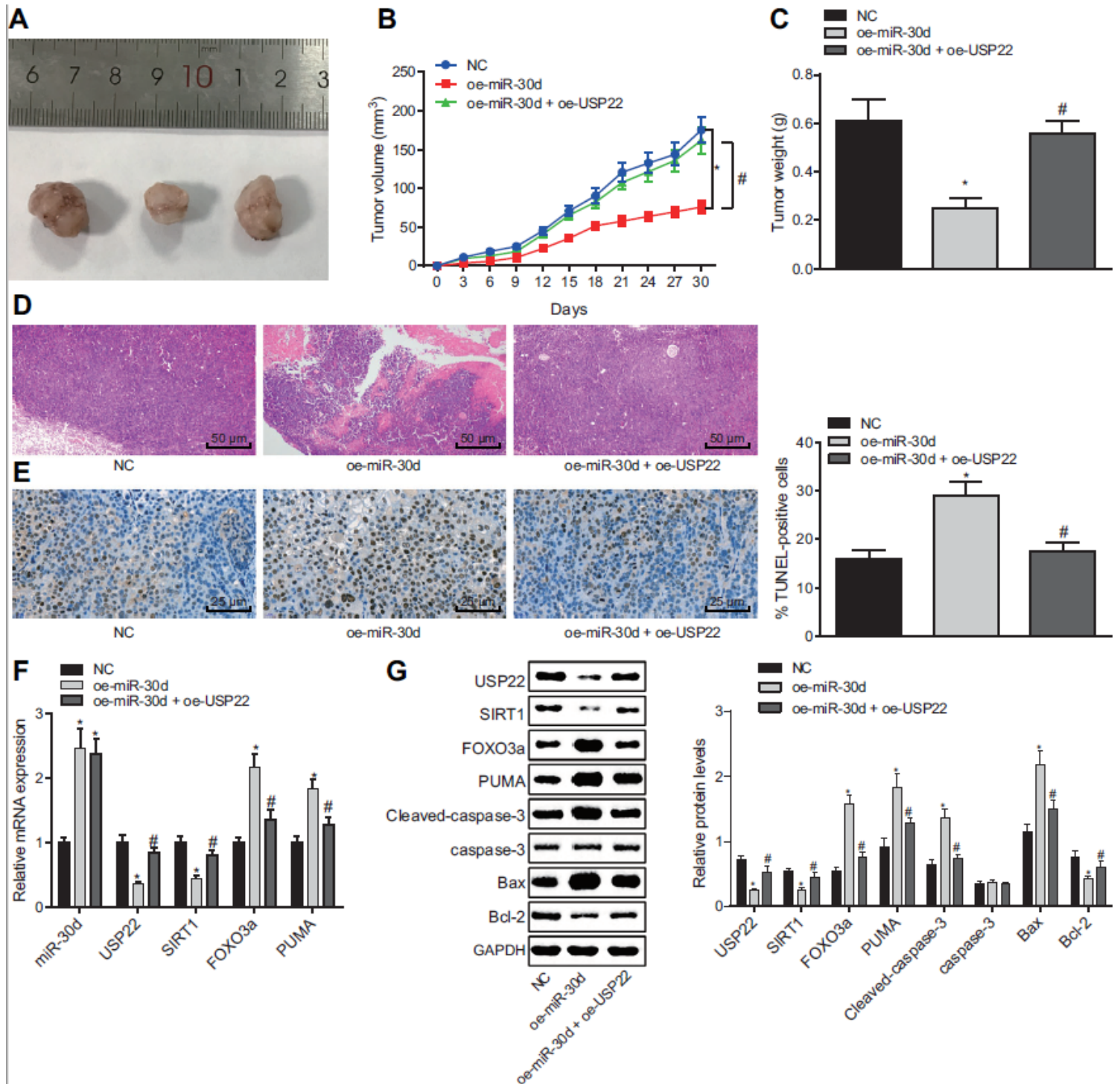

Figure 7

The development of thyroid cancer was restrained by miR-30d by mediating the SIRT1/FOXO3a/PUMA axis through USP22 inhibition. A, Representative pictures of subcutaneously transplanted tumors of nude mice after 30 d. B, Volume of subcutaneously transplanted tumors in nude mice. C, Weight of subcutaneously transplanted tumors in nude mice. D, Tumor lesions of nude mice observed by HE

staining (× 200). E, Cell apoptosis in tumor tissues assessed by TUNEL staining (× 400). F, The expression of miR-30d, USP22, SIRT1, FOXO3a and PUMA in the tumor tissue of mice determined by RT-qPCR. G, The protein expression of USP22, SIRT1, FOXO3a, PUMA, Cleaved-caspas-3, caspase-3, Bcl-2 and Bax in the tumor tissues of mice determined by Western blot analysis. * $p < 0.05$ vs. mice experienced injection of cells stably infected with NC, # $p < 0.05$ vs. mice experienced injection of cells stably infected with miR-30d mimic. The experiment was repeated 3 times, and the analysis of data among multiple groups was performed by one-way ANOVA. Comparison of data at different time points was analyzed using repeated measurement ANOVA.
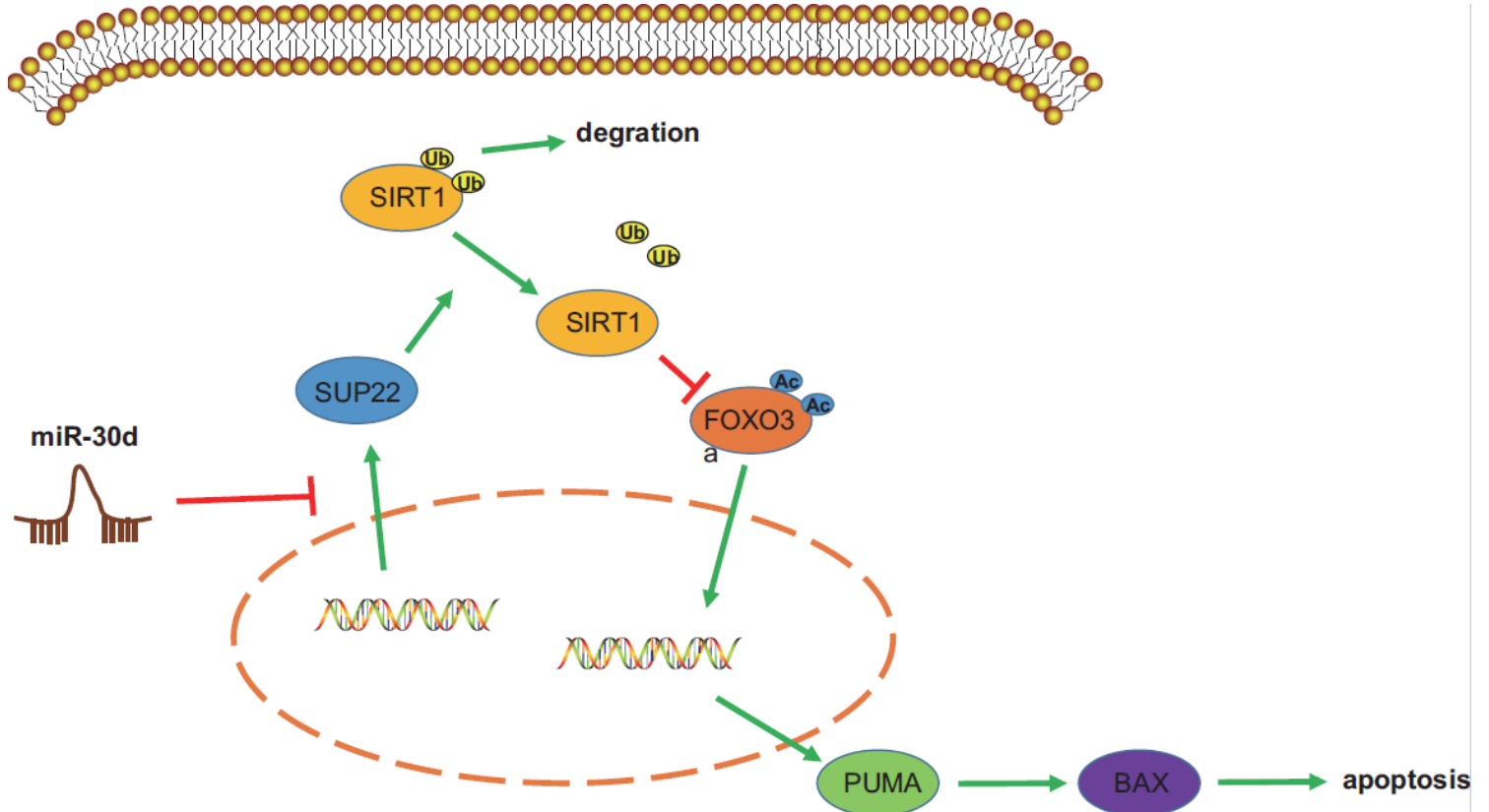

Figure 8

The miR-30d-mediated mechanism involved in the progression of thyroid cancer.